Cross-Stream Migration of Bead–Spring Polymers in Nonrectilinear Pore Flows

Ludwig C. Nitsche
Dept. of Chemical Engineering, The University of Illinois at Chicago, Chicago, IL 60607

Deterministic cross-stream migration of FENE dumbbells, cyclic trimers and bicyclic tetramers in nonhomogeneous, nonrectilinear flows representative of tortuous pores is analyzed. Identifying the crucial feature of misalignment between a tumbling dumbbell and the surrounding streamlines, Brunn (1983) showed that the dumbbell model requires three reflections in the bead–bead hydrodynamic interaction (HI) for lateral migration to occur: lower-order approximations of the HI are insufficient because they lead only to alignment with the flow rather than tumbling. In any orientation the trimer (tetramer) has at least two (three) "bonds" out of alignment with the flow. Radial migration in rotary Couette flow between concentric cylinders occurs in the freely draining limit, and the simplest, first-order HI is sufficient to cause lateral migration in rectilinear tube flow. Flow through a sinusoidally corrugated pore brings a new convective timescale on which the bead–spring entity moves between converging and diverging flow environments. Since this process outpaces the dumbbell's alignment, even a freely draining dumbbell spends most of its time slightly misaligned with the surrounding streamlines, and migrates toward the walls (higher shear). Tumbling occurs on a much longer timescale, with the dumbbell traveling through many wavelengths of the wall corrugations (and fluctuating in orientation) between successive (rapid) end-for-end flips in the shear field. The flipping time seems to scale inversely with the length of the dumbbell. The trimer and tetramer rotate largely as in rectilinear shear, and exhibit somewhat stronger migration for the same bond length. As a simple model of pore entrance effects, net drift in an oscillatory Sampson flow through a thin orifice is also considered.

Introduction

This article addresses the migration of deformable macromolecules across streamlines in nonhomogeneous flows, emphasizing the converging–diverging geometry of porous microstructures. Cross-stream migration is an important determining factor in the spatial distribution of dissolved polymers, and thereby affects the rheology and transport properties of flowing polymer solutions. A number of effects have been explained on this basis, including macromolecular fractionation in capillaries and slip at walls. The direction of migration relative to spatial variations in shear may depend upon the specific flow field: migration toward lower shear has usually been suggested for rectilinear tube and channel flow, whereas migration toward higher shear accompanies rotating-cylinder Couette flow. Inward migration also occurs in Couette flow between concentric cones. These phenomena have received much attention in the literature (Shafer, 1974; Shafer et al., 1974; Aubert and Tirrell, 1980a; Aubert et al., 1980; Brunn, 1983; Brunn and Chi, 1984; Dutta and Mashelkar, 1985; Agarwal et al., 1994).

Theoretical investigations thus far have mainly employed a rheological perspective, whereby the lengthscale of inhomogeneities in the flow is much greater than the characteristic dimension of the dissolved polymers. The former is characterized by a local quadratic component, corresponding to second-order terms in the Taylor expansion. Approached from the perspective of deterministic motion or kinetic theory, the problem is typically one of obtaining the *local* migration velocity (Aubert and Tirrell, 1980a; Aubert et al., 1980; Brunn and Chi, 1984; Bhave et al., 1991). Freely draining elastic dumbbells are the predominant macromolecular model

(Shafer et al., 1974; Aubert and Tirrell, 1980a; Aubert et al., 1980; Bhave et al., 1991; Larson, 1992), but refinements have been advanced to include bead–bead hydrodynamic interactions (HI) and multibead chains (Shafer, 1974; Brunn, 1983, 1984, 1985a; Brunn and Grisafi, 1985b; Jhon and Freed, 1985; Jhon et al., 1987).

Previous work on wall effects in the kinetic theory of polymer solutions has mainly been restricted to flat (or locally flat) walls and rectilinear flows (Brunn, 1976; Aubert and Tirrell, 1982; Stasiak and Cohen, 1983; Park and Fuller, 1984; Goh et al., 1985a–c; Brunn, 1985b; Brunn and Grisafi, 1985a, 1987a,b; Grisafi and Brunn, 1989)—sometimes with more comprehensive accounting for geometric aspects of confinement in pores than for bead–wall hydrodynamic interactions. Contributions that address hydrodynamic wall effects with reference to migration include Jhon and Freed (1985) and Jhon et al. (1987). The influence of far-field spatial velocity fluctuations on polymer stretching in dilute beds has been analyzed by Shaqfeh and Koch (1992).

In the asymptotic limit of small macromolecules situated a pore-scale distance away from the walls, hydrodynamic wall effects represent a higher-order correction compared with the bead–bead interactions (cf. Jhon and Freed, 1985), and steric constraints do not arise. Thus, we shall not explicitly account for hydrodynamic or steric wall effects, for which one would actually need to specify the scale of pore-wall roughness relative to the macromolecular size (cf. Goh et al., 1985a). Implicitly, of course, the confining walls determine the flow field in which the bead–spring polymer moves.

Here we revisit the problem of cross-stream migration in *nonrectilinear* pore geometries, for which there arises a crucial convective timescale on which dissolved entities are carried from one inhomogeneous flow environment to another. This *Lagrangian unsteadiness* has long been recognized as crucial to the rheology of polymer solutions in porous media (Deiber and Schowalter, 1981; Phan-Thien and Khan, 1987; Vorwerk and Brunn, 1991). The impact of this feature upon lateral migration has received much less attention, although the importance of curved streamlines—in rotary Couette flow and in porous geometries—has been pointed out: the effect is migration toward the concave side (Shafer, 1974; Shafer et al., 1974; Aubert and Tirrell, 1980a,b; Aubert et al., 1980; Brunn, 1983). Because the flow is faster in the smaller cross sections, the bead–spring entities spend less time in the outwardly concave streamlines of the pore throats than in the inwardly concave streamlines of the pore bodies. Nevertheless, we shall find the net (deterministic) migration in a sinusoidally corrugated pore to be away from the axis.

The scenario of macromolecules that are not negligible in size compared with the surrounding pores arises in hindered membrane transport, macromolecular fractionation and enhanced oil recovery (Deen, 1987; Davidson and Deen, 1988; Guillot et al., 1985; Gogarty, 1967; Chauveteau, 1982). For this size regime the distinction between strong and weak flows (Rallison and Hinch, 1988) may lose importance, simply because linearly elastic dumbbells will not have sufficient time to stretch greatly relative to their undeformed length in elongational, converging flows (entering pore throats) before reaching the diverging flows (entering pore bodies).

Our investigation of purely deterministic lateral migration is *not* advanced by way of *neglecting* Brownian motion. Rather, we seek to elucidate and systematize the relation between structural and hydrodynamic features of a bead–spring polymer model and resultant convective mechanisms of cross-stream migration, information that would represent the deterministic *input* to a (subsequent, more comprehensive) kinetic theory of convective–diffusive transport. This was the essential spirit of the paper by Brunn (1983), which was later followed up with kinetic theory (Brunn and Chi, 1984). Main new elements here in relation to the deterministic work of Brunn are (1) the extension to *nonrectilinear* flow in a sinusoidally corrugated pore and in an orifice, and (2) somewhat more complicated bead–spring arrangements.

Each bead in the bead–spring entity disturbs the fluid, thereby contributing, in a mutually coupled manner, to the fluid environment experienced (and disturbed) by all the other beads. An important simplification is possible in the limit of small bead radius a compared with the minimum distance l between any two beads. In an asymptotic hierarchy, the most important disturbances come from *relative translational motions* that arise because the (freely suspended) entity straddles spatial variations of the suspending flow field. As a first approximation, this effect can be modeled by regarding each bead as a shapeless "point force" pushing against the fluid, which disturbs all other beads at order $O(a/l)$. Although each point force indirectly influences its own incident field through back reflections from the other beads, such contributions appear only as higher corrections. Thus, at leading order the individual bead velocities become decoupled (in a manner to be made precise below in the Dynamic Equations section). This is the essence of the *first-order* approximation to HI. Higher-order HI, constituting a hierarchy of increasingly accurate refinements, account for successive back reflections as well as more subtle effects associated with shape and rigidity (Kim and Karrila, 1991, Chap. 8). For example, to model the tumbling of a dumbbell in simple shear flow one must consider three reflections (Brunn, 1983).

Using a FENE dumbbell model, Brunn (1983) established the two crucial requirements for deterministic cross-stream migration: (1) deformability, and (2) bead–bead hydrodynamic interactions. More precisely, it was the *higher-order* HI that caused the dumbbell to tumble in the (local) shear field; net drift normal to the streamlines then resulted from a (constantly changing) misalignment between the elastic dumbbell's axis and the flow direction. Brunn considered rectilinear channel flow and Couette flow between concentric cylinders. For both cases it is important to emphasize that first-order HI (involving only Stokeslet interactions but no reflections) are insufficient for lateral migration of a dumbbell because they lead only to a terminal alignment with the local flow.

In order to more clearly separate the operative phenomena, here we shall use polymer models that rotate in shear flow *even in the freely draining limit* in which HI are entirely neglected. Positioned on a meridian plane of an axisymmetric flow (or parallel to the plane of a two-dimensional flow), the cyclic timer and bicyclic tetramer illustrated in Figure 1 (cf. Bird et al., 1987, Chap. 16; Bloomfield and Zimm, 1966) both rotate in any orientation relative to the local shear field, due to their noncolinear friction centers. (In order to achieve tumbling motion in all possible orientations relative to a general three-dimensional flow field, it would be sufficient to consider a tetrahedral assembly.) With these models, simple

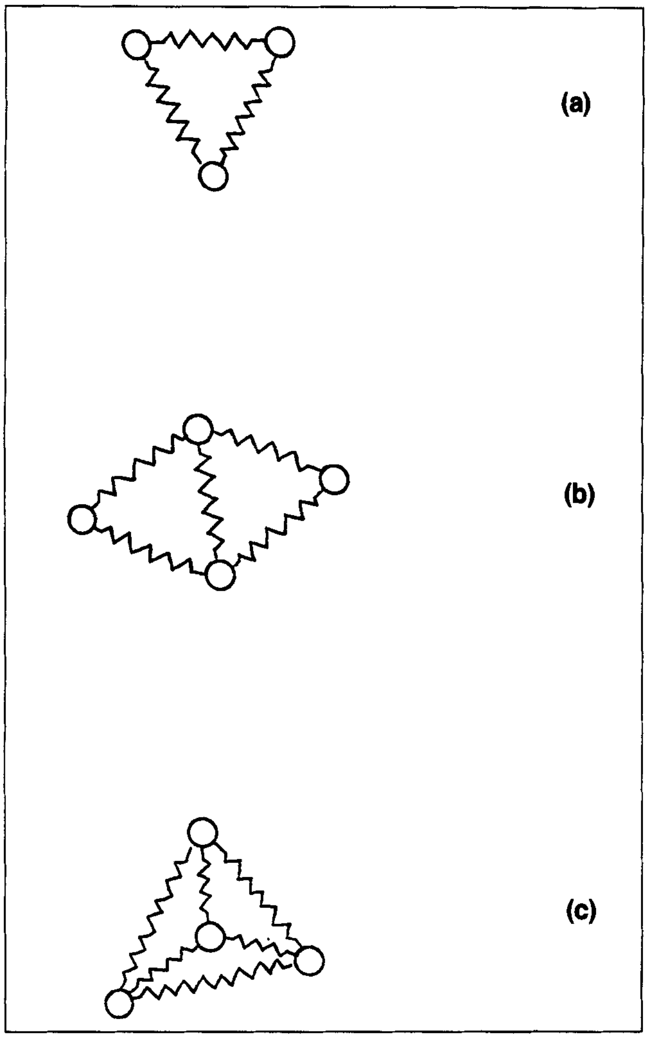

Figure 1. Simple bead-spring models of polymers that tumble in shear flow even in the freely draining limit.

(a) Cyclic trimer. (b) Bicyclic tetramer. (c) Tetrahedral assembly.

first-order HI (which would *not* cause a dumbbell to tumble in shear) will be seen to suffice for lateral drift in rectilinear tube flow.

Most importantly for applications in porous-media flows, we will show that even a *freely draining dumbbell* undergoes deterministic migration toward the walls of a sinusoidally corrugated pore. Because the dumbbell keeps moving *between* different inhomogeneous flow environments, with insufficient time to adjust to each local environment, *it spends most of its time slightly misaligned with the converging–diverging streamlines*, and therefore undergoes lateral migration. Tumbling does occur, but by a different mechanism than the higher-order HI effect in simple shear flow, as discussed below. The curved streamlines in Couette flow between *coaxial* cylinders are not enough for lateral migration of a freely draining dumbbell. There must also be *streamwise changes in the cross section*, which would, however, be the case for eccentric cylinders (journal-bearing flow).

In the stochastic realm of kinetic theory, Brownian fluctuations contribute to the crucial misalignment between the flow and the dumbbell, and lateral migration has also been explained using entropic arguments (see Shafer et al., 1974; Tirrell and Malone, 1977; Aubert and Tirrell, 1980a; Brunn, 1983). Furthermore, Sekhon et al. (1982) have shown that first-order HI are sufficient in combination with Brownian motion for lateral migration of a dumbbell to occur in rectilinear flow. [This was not the case for deterministic motion (Brunn, 1983).] The preceding observations are summarized in Table 1 (cf. Agarwal et al., 1994, Table 3).

Dynamic Equations

The equations of motion for a bead–spring macromolecule are summarized below, assuming creeping flow and negligible inertia of the beads, along the lines of Bird et al. (1987, secs. 13.6, 14.6, 15.4). Furthermore, we do not consider the influence of the suspended entity upon the surrounding flow field. The beads and springs are assumed identical, all being of radius a and undeformed length ℓ, respectively. In considering the asymptotic limit $\ell \to 0$, we hold the (small) ratio $\alpha = a/\ell$ fixed, so as to preserve geometric similarity as the macromolecular entity is shrunk down.

Brunn (1983) devised a convenient force law to keep the spring length within fixed limits of stretching and compression (finite extensibility and excluded volume; see below). For our calculations involving the models in the first two parts of Figure 1, this means that the distance between any two beads is always of order ℓ. The total spring force $\boldsymbol{F}_\mu$ on each bead, μ, must balance the hydrodynamic friction,

$$\boldsymbol{F}_\mu = \zeta_0 \left[\dot{\boldsymbol{R}}_\mu - \boldsymbol{V}_\mu \right], \tag{1}$$

with $\zeta_0 = 6\pi\eta\,\ell\alpha$ the Stokes'-law friction coefficient, and $\boldsymbol{V}_\mu$ the fluid approach velocity felt at the center $\boldsymbol{R}_\mu$ of bead μ.

Table 1. Cross-Stream Migration Behavior of Dumbbells and Cyclic Trimers Under Various Conditions*

	Deterministic			Brownian Motion	
Bead–Spring Model	Rectilinear	Concentric Cylinder	General Curvilinear	Rectilinear	Curvilinear
Dumbbell, freely draining	No	No	Yes	No	Yes
Dumbbell, first-order HI	No	No	Yes	Yes	Yes
Dumbbell, higher HI (3 reflections)	Yes	Yes	—	Yes	—
Cyclic trimer, freely draining	No	Yes	Yes	—	—
Cyclic trimer, first-order HI	Yes	Yes	Yes	—	—

Source: Based on this work as well as conclusions drawn from Shafer (1974), Shafer et al. (1974), Aubert and Tirrell (1980a), Sekhon et al. (1982), and Brunn (1983, 1984).

*Yes = presence; No = absence.

Motion of the beads relative to the surrounding fluid arises because the freely suspended assembly straddles variations in velocity given by the characteristic gradient scale U/L and the polymer's characteristic lengthscale ℓ. Thus, the characteristic scale of frictional force on one bead is

$$\mathfrak{F} = U(\ell/L)\eta\alpha\ell. \tag{2}$$

If one neglects bead–bead HI entirely, then V_μ is simply the undisturbed fluid velocity v evaluated at R_μ. The first HI correction comes from the bead–fluid relation motion, whose contribution to the approach velocities is captured at this order by the resulting Stokeslet (point-force) fields of characteristic strength $\mathfrak{F}$ that act over distances of order ℓ upon the other beads:

$$V_\mu = v(R_\mu, t) + \sum_{\nu \neq \mu} \mathcal{G}(R_\mu - R_\nu)\cdot F_\nu. \tag{3}$$

Here $\mathcal{G}$ is the Oseen tensor,

$$\mathcal{G}(R) = \frac{1}{8\pi\eta\|R\|}\left\{I + \frac{RR}{\|R\|^2}\right\}. \tag{4}$$

This is often replaced with the Rotne–Prager–Yamakawa tensor,

$$\mathcal{G}_{RPY} = \frac{1}{8\pi\eta\|R\|}\left\{\left(1 + \frac{2}{3}\alpha^2\right)I + (1 - 2\alpha^2)\frac{RR}{\|R\|^2}\right\}, \tag{5}$$

in kinetic theory and Brownian dynamics simulations in order to avoid negative diffusivities of longer chains. In this connection see the discussion in Bird et al. (1987, sec. 14.6) in relation to the original references (Rotne and Prager, 1969; Yamakawa, 1970); see also Rey et al. (1989) and Rudisill and Cummings (1992).

Thus, for a freely suspended bead–spring polymer we have the following coupled system of nonlinear ordinary differential equations:

$$\dot{R}_\mu = v(R_\mu) + \zeta_0^{-1}F_\mu(Q) + \sum_{\nu \neq \mu} \mathcal{G}(R_\mu - R_\nu)\cdot F_\nu(R) + \text{wall effects} \tag{6}$$

$$= O(U) + O[U(\ell/L)] + O[U\alpha(\ell/L)] + O[U\alpha(\ell/L)^2]. \tag{7}$$

The contribution of HI (third term) to the approach velocity is small compared with the slip velocity due to the springs (second term) because we assume the reduced bead radius α to be small. However, the small value of α stays fixed in the asymptotic limit $(\ell/L) \to 0$, so these two effects are both formally of first order in (ℓ/L). The magnitude of wall effects just indicated can be bounded using the frictional force scale $\mathfrak{F}$ acting over distances of order L through the Stokeslet fields to produce velocity disturbances of order $O(\mathfrak{F}\eta^{-1}L^{-1})$ on the walls; the resultant reflected fields contribute at the same order to the approach velocities V_μ felt by the beads. It should be pointed out that, on a *relative* basis, wall effects do influence the HI terms more strongly than the slip terms. In neglecting wall effects in our computations of cross-stream migration, we would therefore seem to commit a greater error in cases where HI are actually *necessary* for lateral migration, and do not just play a contributory role (Table 1).

We use the symbol $Q = \{R_\mu\}$ to denote the collection of all bead position vectors, thereby recognizing that the spring force on each bead can in general depend upon the (relative) positions of all beads. The arrangement of the springs is summarized by the bond matrix $C_{\mu\nu}$, whose entries are unity for distinct beads μ and ν that are connected, and vanish otherwise.

$$F_\mu(Q) = \sum_{\nu \neq \mu} C_{\mu\nu} f(\|R_\nu - R_\mu\|)\frac{R_\nu - R_\mu}{\|R_\nu - R_\mu\|}. \tag{8}$$

As written here, the nonlinear force law of Brunn (1983) keeps the spring length within the fraction ψ of its undeformed value; the reduced stiffness constant κ is referred to the viscous force scale,

$$f(d) = \kappa\zeta_0(d - \ell)\left[1 - \left(\frac{d - \ell}{\psi\ell}\right)^2\right]^{-1}. \tag{9}$$

Computations of Cross-Stream Migration

The calculations presented below were carried out with the reduced bead radius $\alpha = 0.05$; the nonlinear spring parameter $\psi = 0.5$ was used to keep all bond distances between $\ell/2$ and $3\ell/2$. We used $\kappa = 1.0$ for the reduced spring constant. Bead–bead hydrodynamic interactions were incorporated using the Oseen tensor (as opposed to the Rotne–Prager–Yamakawa tensor). The characteristic linear dimension L was normalized to unity. This represented the radius of the straight tube, the maximum radius of the corrugated tube, the radius of the orifice, and the radius of the outer cylinder in rotary Couette flow. On this basis of nondimensionalization, we used two values of the equilibrium spring length ($\ell = 0.025$ vs. $\ell = 0.05$) chosen as a compromise between (1) ℓ sufficiently small for reasonable anticipated accuracy with regard to neglected hydrodynamic wall effects (at least for qualitative mechanistic conclusions), and (2) ℓ sufficiently large for readily observable migration. Without accounting for the hydrodynamic wall effects, and with no additional repulsive potentials, the polymers models would eventually run through the walls. In each geometry the flow field was normalized for unit cross-sectional-average or volume-average velocity, depending upon which was applicable. A fourth-order Runge–Kutta scheme was used to integrate the coupled equations of motion for the various flow fields, with the time step $\Delta t = 0.001$; accuracy and stability of the trajectories was spot checked by doubling Δt. Once started in a meridian plane of the axisymmetric tube, corrugated pore, or orifice, the bead–spring entity could not leave this plane. Similarly, motion in the rotary Couette flow was confined to a plane normal to the axis. (The numerics were general, and did not take advantage of this feature.)

Figure 2 shows the trajectories of the centroid for cyclic trimers and bicyclic tetramers in rectilinear flow through a

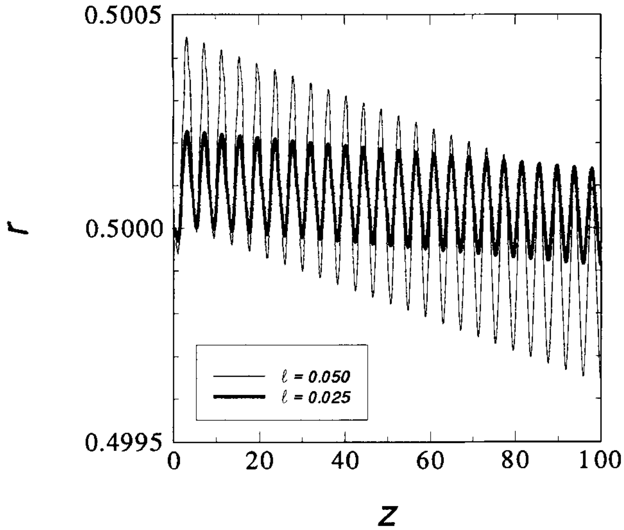

(a)

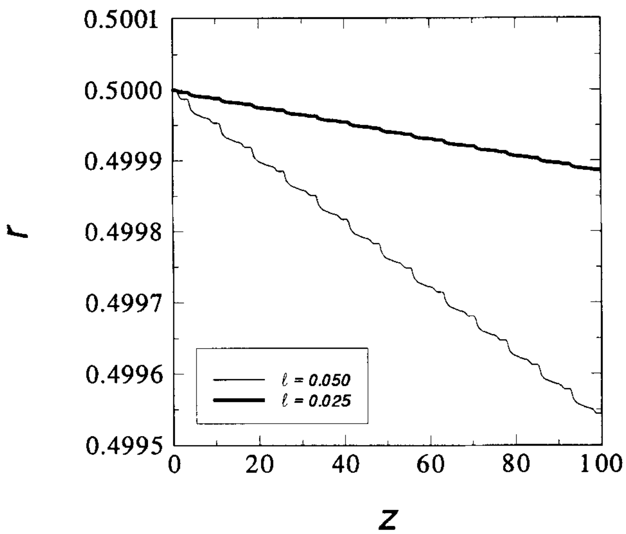

(b)

Figure 2. Center-of-mass trajectories for bead-spring polymers carried along by Poiseuille flow in a straight circular tube of unit (dimensionless) radius.

Each graph shows the relationship between axial (z) and radial (r) motion in a meridian plane, to which the model polymer is confined by virtue of its initial condition. First-order hydrodynamic interactions together with elasticity lead to net migration toward the axis. (a) Cyclic trimers. (b) Bicyclic tetramers.

circular cylindrical tube of unit (dimensionless) radius. In both cases the periodic fine structure is associated with the tumbling motion that is superimposed upon net drift toward the axis accompanying each revolution, which occurs here for *first-order* HI between the beads. Per unit axial distance traveled, the net radial migration is only about 0.0015 ℓ^2 for the trimer vs. 0.0018 ℓ^2 for the tetramer. Thus, even after being carried downstream a distance of 100 tube radii, the total radial drift is still small compared with the characteristic polymer lengthscale ℓ. In qualitative features and in the rough magnitude of the drift effect, these graphs agree with the results of Brunn (1983) for a dumbbell with higher-order HI (required for it to tumble in shear). In particular, we reproduce (as we must) the expected ℓ^2 scaling of the lateral migration velocity with other geometric parameters held fixed. In the absence of HI, the centroid of the trimer or tetramer does not fluctuate radially at all while it moves in the axial direction with the beads rotating around it (see Figure 7, to be discussed later). A freely draining dumbbell, or one with first order HI, does not migrate laterally, because it simply becomes aligned with the flow.

Inward migration of the cyclic trimer in rotary Couette flow (outer cylinder stationary, inner concentric cylinder rotating counterclockwise) is depicted in Figure 3. This is due essentially to the curved streamlines, and is two or three orders of magnitude faster than lateral migration in rectilinear tube flow (pure HI effect): per unit circumferential distance traveled, the net migration is (within an estimated precision of 0.01 in the coefficients) 0.76 ℓ^2 in the freely draining case vs. 0.79 ℓ^2 with first-order HI. The difference, attributable to HI, is substantially larger than the *total* drift in the rectilinear tube flow. In considering the additional circumferential distance traveled by the trimer in the presence of HI (Figure 3b), we note that it would seem difficult to separate any direct streamwise migration (in connection with kinetic theory, see, e.g., Aubert and Tirrell, 1980a; Jhon et al., 1987) from the effect of inward migration toward faster streamlines.

For the sinusoidally corrugated pore from Figure 4, the axisymmetric Stokes flow field is calculated with a least-squares boundary singularity method, slightly modified from Nitsche and Brenner (1990). We denote by θ the angle between the dumbbell axis and the fluid velocity vector evaluated at its midpoint (Figure 5). Because the polymer model stays in the (y, z) meridian plane, this angle is computed here according to the formula

$$\theta = \text{Arcsin}\left[\frac{(Y_2 - Y_1)v_z - (Z_2 - Z_1)v_y}{\|\boldsymbol{R}_2 - \boldsymbol{R}_1\| \, \|\boldsymbol{v}\|}\right]. \qquad (10)$$

With θ thus confined to the interval $[-90°, 90°]$, successive spikes reaching $\pm 90°$ actually represent an incremental rotation through 180°.

Figure 6a shows trajectories of *freely draining* dumbbells in the corrugated pore. In the (z, r) meridian plane, the low and high points of the trajectory are compared with the corresponding bounds for the fluid streamline that passes through the initial location of the center of mass. The angle θ is plotted as a function of axial distance traveled in Figure 7a. For a freely draining dumbbell the converging–diverging nature of the flow is crucial for rotation, because in a rectilinear flow field it would simply become aligned with the streamlines. Here the dumbbell is carried between pore throats and bodies faster than it can align with any local flow environment. Thus, it rocks between more and less closely aligned orientations—fluctuating about a gradually increasing misalignment —while traveling through many pore wavelengths. This continues until the dumbbell protrudes sufficiently far perpendicular to the flow direction for the local shear field to quickly flip it end-for-end (Figure 5). Thus, there exists a vague analogy with Jeffery orbits of slender bodies (or dumbbells with

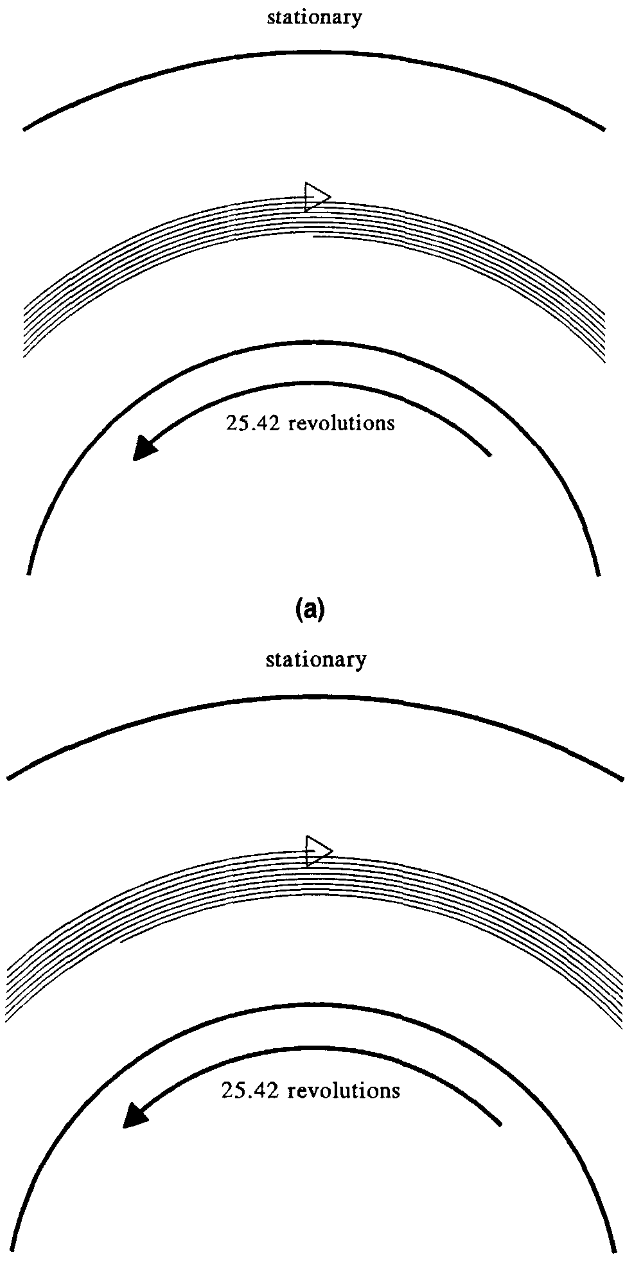

Figure 3. Center-of-mass trajectories for cyclic trimers in rotary Couette flow between concentric cylinders.

The outer cylinder is stationary, while the inner cylinder has made 25.42 revolutions in the counterclockwise direction. In each case the triangle indicates the trimer's size ($\ell = 0.05$) and initial position and orientation. (a) Freely draining. (b) First-order HI.

higher-order HI) in shear flow (Kim and Karrila, 1991, sec. 5.5.2), where the fastest vs. slowest angular velocities correspond to orientations orthogonal vs. parallel to the streamlines, respectively. The flipping distance seems to scale like ℓ^{-1}; we expect the associated constant to be determined by the closeness of the trajectory to the wall.

Lateral migration behavior of the freely draining cyclic trimers and bicyclic tetramers in the sinusoidally corrugated

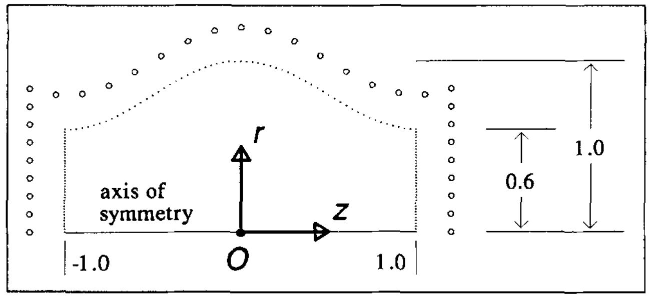

Figure 4. Dimensionless unit cell for a sinusoidally corrugated pore with wavelength 2 and constriction ratio 0.6 referred to unit maximum radius.

With reference to the least-squares boundary singularity method (Nitsche and Brenner, 1990), open circles mark the positions of ring singularities, and closed dots indicate the points at which the no-slip or periodic boundary conditions are imposed in a least-squares sense to determine the unknown coefficients of the singular basis functions.

pore is depicted in Figures 6b and 6c, respectively. With reference to tumbling of the freely draining FENE dumbbell in the sinusoidally corrugated pore (Figure 7a), a more recent article (Nitsche, 1996) considers similar rotary dynamics of a *rigid* dumbbell from both numerical and asymptotic points of view. In particular, a two-scale analysis, combined with lubrication theory, yields an analytical approximation for the early stages of the fluctuating misalignment with the flow and motivates the numerically observed ℓ^{-1} scaling of the distance traveled between successive end-for-end flips. With reference to Figures 7b and 7c, the orientation of trimer or tetramer is specified by basing the angle θ upon one bond (chosen arbitrarily for reference) and the fluid velocity vector evaluated at the center of mass of the whole entity. Tumbling is seen to occur largely as in rectilinear tube flow, but with additional

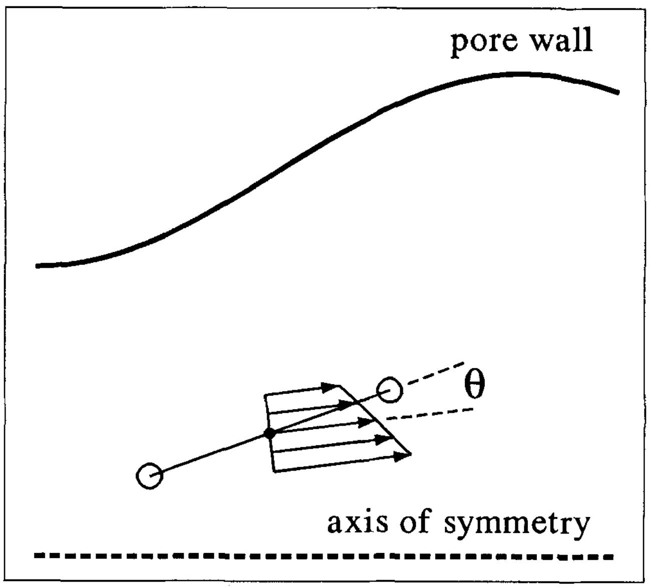

Figure 5. Orientation (angle θ) of a dumbbell relative to the surrounding streamlines.

When the dumbbell protrudes sufficiently far normal to the flow direction, the local shear field quickly flips it end-for-end—corresponding to one of the spikes in Figure 7a. Here the size of the dumbbell is greatly exaggerated.

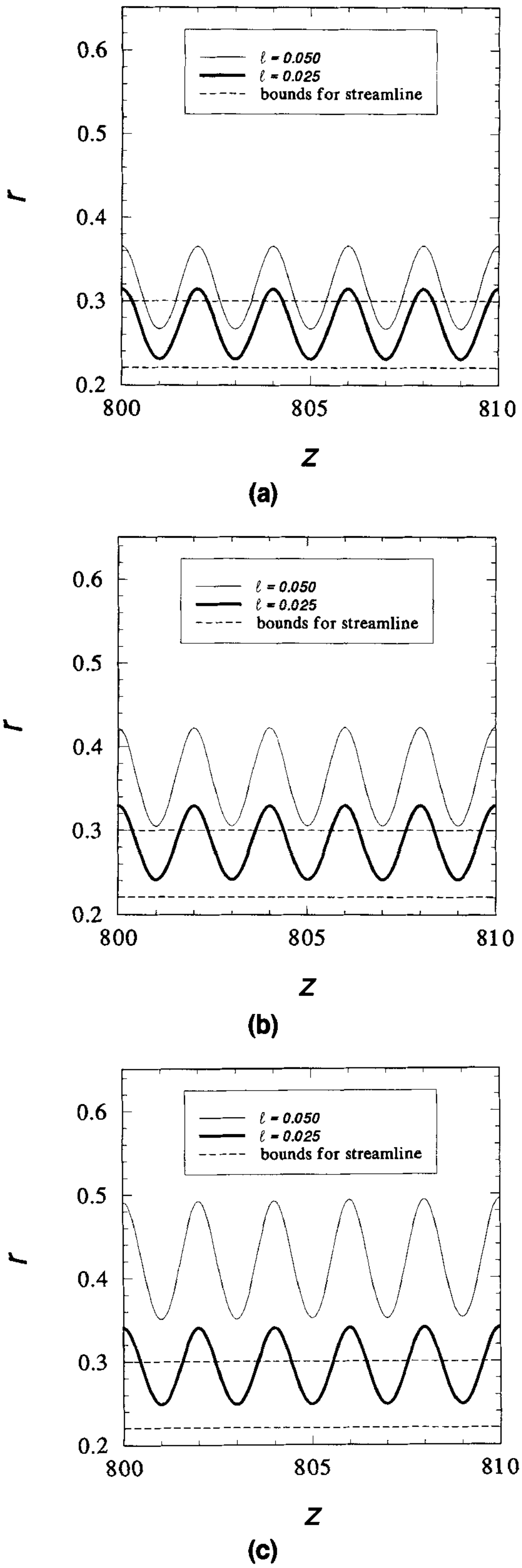

Figure 6. Center-of-mass trajectories for freely draining bead–spring polymer models carried along in a meridian plane by the flow through the sinusoidally corrugated pore from Figure 4.

Here the bead–spring entity starts with its center of mass at $(z, r) = (0, 0.3)$. (a) Dumbbell. (b) Cyclic trimer. (c) Bicyclic tetramer.

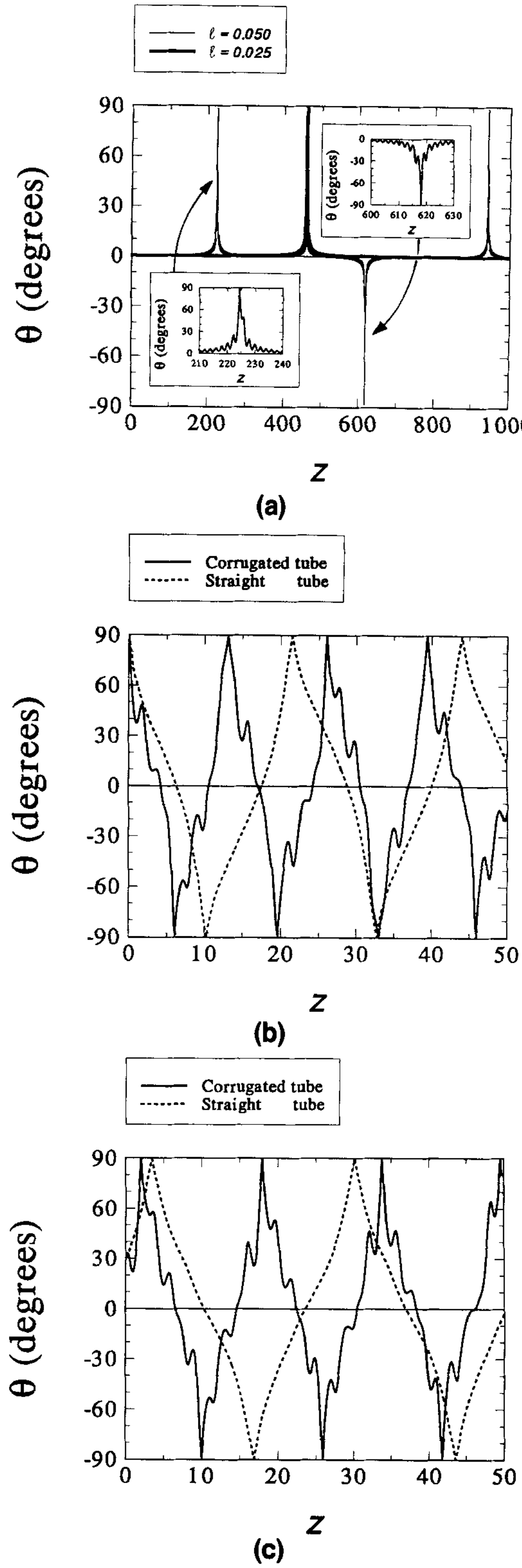

Figure 7. Orientation (angle θ between the 1–2 bond and fluid velocity vector evaluated at the center of mass) of freely draining bead–spring polymer models as a function of axial distance traveled (cf. Figure 6) through the corrugated pore from Figure 4.

The same initial position, $(z, r) = (0, 0.3)$, is used for flow through the straight tube of unit radius.

Table 2. Approximate Scaling Constants B for Cumulative Radial Migration Divided by the Axial Distance Traveled in Figure 6 (800–810 Radii) by Freely Draining Bead–Spring Entities in the Sinusoidally Corrugated Pore: (Radial Migration)/(Axial Distance) $\approx B\ell^2$

Bead–Spring Model	B_L	B_H	Precision (Est.)
Dumbbell	0.020	0.028	0.005
Cyclic trimer	0.041	0.058	0.004
Bicyclic tetramer	0.056	0.080	0.016

Note: In a (z,r) meridian plane, the low (L) and high (H) points of the trajectory are compared with the corresponding bounds for the fluid streamline that passes through the initial location, $(z,r)=(0,0.3)$, of the center of mass.

fine structure in the orientational trajectory. With reference to Figure 6 and Table 2, we note that migration toward the wall becomes stronger as we add more beads to the polymer model.

We shall use the Sampson flow through a circular orifice in an infinitesimally thin plate (Happel and Brenner, 1983, sec. 4-29; Davis, 1991) as a very simple idealization of the flow field near the mouth of one pore in a membrane. In Figure 8 we investigate the net migration of a cyclic trimer in oscillatory, *zero-mean* flow through the orifice. [Citing weak lateral drift in rectilinear flow, Brunn (1983) has suggested that prolonged oscillatory flow could lead to more readily observable effects.] Cross-stream migration toward the concave side and (apparent) streamwise drift both push the trimer toward the edge of the orifice. By causing deformable macromolecules to undergo net migration, it is conceivable that oscillatory flow could perhaps influence the overall transport resistance of macromolecules through comparatively much larger pores, thereby creating an externally controllable "diffusion gate." If species-selectivity of the drift effect (based upon macromolecular size, shape or flexibility or elasticity) turns out to be appreciable, it could be useful for membrane separations.

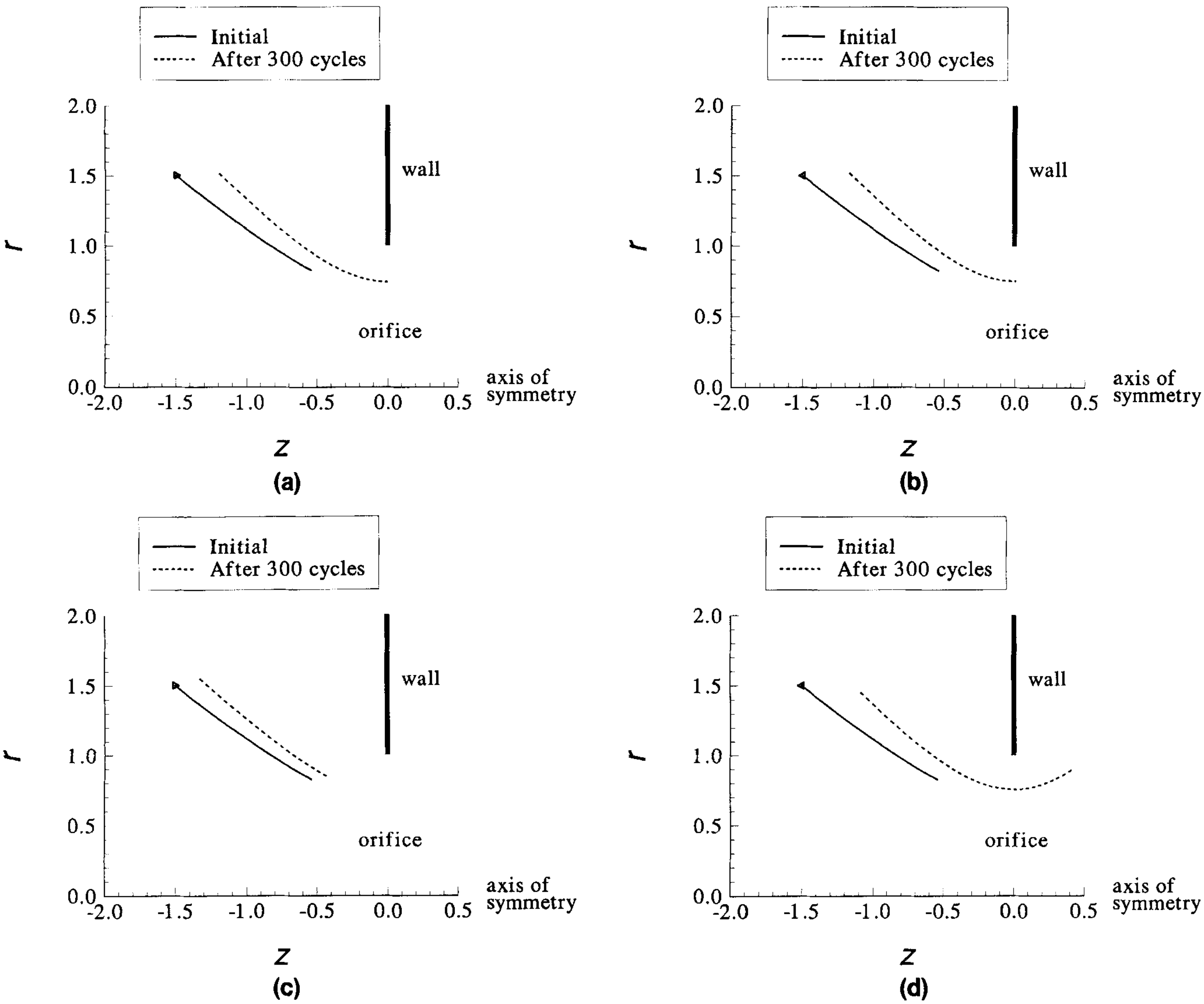

Figure 8. Center-of-mass trajectories of cyclic trimers in zero-mean oscillatory flow through an orifice.

Each curve represents motion in one direction of a cycle (period $T=12.5$) of the flow. In each case the triangle indicates the trimer's size ($\ell=0.05$) and its initial position and orientation (in a meridian plane) relative to the perforated flat wall. The latter, seen edge-on, lies perpendicular to the z-axis. (a) and (b) Freely draining. (c) and (d) First-order HI.

(This aspect will be investigated in a subsequent article.) In the case of bead–bead HI (Figures 8c and 8d) one notices a curious sensitivity of the long-time trajectory to the initial *orientation* of the trimer (for the same starting centroid position).

Concluding Remarks

The calculations presented here underscore the importance of realistically capturing the converging–diverging nature of flow fields when one considers cross-stream migration of flexible polymers in porous media. Even in the purely deterministic cases studied here, the concept of *local* migration velocity is seen to have two significant limitations: (1) realistic applications do not always admit the usual assumption of widely separated macromolecular vs. pore lengthscales; and (2) even for very small suspended entities, convection *between* pore throats and bodies seems to outpace the lateral migration mechanisms advanced for simpler nonhomogeneous flows.

For bead–spring polymer models sufficiently small to justify (at least to a reasonable approximation) the neglect of hydrodynamic wall effects, the migration phenomena illustrated above have been quite weak. Stronger effects for larger macromolecular entities can be inferred partly from the expected ℓ^2 scaling of the migration velocity; for, it is reasonable to suppose that corrections due to the walls would not drastically alter qualitative aspects of the trajectories.

The deterministic convective effects observed here have a rich structure even for the simplest bead–spring model of a polymer, the freely draining dumbbell. These features could have significant ramifications for subsequent kinetic theory applied to the same flow fields.

Acknowledgment

Financial support from the National Science Foundation (grant CTS-9210277) is gratefully acknowledged. The author would also like to thank two anonymous referees for helpful suggestions.

Notation

B = scaling constant describing radial migration in the sinusoidally corrugated pore
d = distance between two beads
f = scalar force exerted by a spring between two beads
T = period of oscillatory flow
U = characteristic flow velocity scale
X, Y, Z = Cartesian coordinates of the bead position vector $\boldsymbol{R}$
η = viscosity of the Newtonian fluid

Subscripts

H, L = local maximum or minimum, respectively, of a center-of-mass trajectory, Figure 6
RPY = Rotne–Prager–Yamakawa tensor
x, y, z = components of a vector

Literature Cited

Agarwal, U. S., A. Dutta, and R. A. Mashelkar, "Migration of Macromolecules Under Flow: The Physical Origin and Engineering Implications," *Chem. Eng. Sci.*, **49**, 1693 (1994).
Aubert, J. H., S. Prager, and M. Tirrell, "Macromolecules in Nonhomogeneous Velocity Gradient Fields: II," *J. Chem. Phys.*, **73**, 4103 (1980).
Aubert, J. H., and M. Tirrell, "Effective Viscosity of Dilute Polymer Solutions Near Confining Boundaries," *J. Chem. Phys.*, **77**, 553 (1982).
Aubert, J. H., and M. Tirrell, "Macromolecules in Nonhomogeneous Velocity Gradient Fields," *J. Chem. Phys.*, **72**, 2694 (1980a).
Aubert, J. H., and M. Tirrell, "On the Origins of Flow-Rate Dependence of Elution Volume in Gel Permeation Chromatography," *Sep. Sci. Technol.*, **15**, 123 (1980b).
Bhave, A. V., R. C. Armstrong, and R. A. Brown, "Kinetic Theory and Rheology of Dilute, Nonhomogeneous Polymer Solutions," *J. Chem. Phys.*, **95**, 2988 (1991).
Bird, R. B., C. F. Curtiss, R. C. Armstrong, and O. Hassager, *Dynamics of Polymeric Liquids*, Vol. 2, *Kinetic Theory*, 2nd ed., Wiley, New York (1987).
Bloomfield, V., and B. H. Zimm, "Viscosity, Sedimentation, *et Cetera*, of Ring- and Straight-Chain Polymers in Dilute Solution," *J. Chem. Phys.*, **44**, 315 (1966).
Brunn, P. O., "Linear Polymers in Nonhomogeneous Flow Fields: II. The Cross-Stream Migration Velocity," *J. Poly. Sci. Poly. Phys. Ed.*, **23**, 89 (1985a).
Brunn, P. O., "Wall Effects for Dilute Polymer Solutions in Arbitrary Unidirectional Flows," *J. Rheol.*, **29**, 859 (1985b).
Brunn, P. O., "Polymer Migration Phenomena Based on the General Bead-Spring Model for Flexible Polymers," *J. Chem. Phys.*, **80**, 5821 (1984).
Brunn, P. O., "Hydrodynamically Induced Cross Stream Migration of Dissolved Macromolecules (Modelled as Nonlinearly Elastic Dumbbells)," *Int. J. Multiphase Flow*, **9**, 187 (1983).
Brunn, P., "The Effect of a Solid Wall for the Flow of Dilute Macromolecular Solutions," *Rheol. Acta*, **15**, 23 (1976).
Brunn, P. O., and S. Chi, "Macromolecules in Nonhomogeneous Flow Fields: A General Study for Dumbbell Model Macromolecules," *Rheol. Acta*, **23**, 163 (1984).
Brunn, P. O., and S. Grisafi, "Wall Effects in Simple Shear of Dilute Polymer Solution: Exact Results for Very Narrow and Very Wide Channels," *J. Non-Newtonian Fluid Mech.*, **24**, 343 (1987a).
Brunn, P. O., and S. Grisafi, "Pressure Driven Flow of Dilute Polymer Solutions in a Channel: Analytic Results for Very Small and for Very Large Channels," *Rheol. Acta*, **26**, 211 (1987b).
Brunn, P. O., and S. Grisafi, "Kinetic Theory of a Dilute Polymer Solution in a Small Channel: Equilibrium Results," *Chem. Eng. Commun.*, **36**, 367 (1985a).
Brunn, P. O., and S. Grisafi, "Linear Polymers in Nonhomogeneous Flow Fields: I. Translational Diffusion Coefficient," *J. Poly. Sci. Poly. Phys. Ed.*, **23**, 73 (1985b).
Chauveteau, G., "Rodlike Polymer Solution Flow Through Fine Pores: Influence of Pore Size on Rheological Behavior," *J. Rheol.*, **26**, 111 (1982).
Davis, A. M. J., "A Translating Disk in a Sampson Flow; Pressure-Driven Flow Through Concentric Holes in Parallel Walls," *Q. J. Mech. Appl. Math.*, **44**, 471 (1991).
Davidson, M. G., and W. M. Deen, "Hydrodynamic Theory for the Hindered Transport of Flexible Macromolecules in Porous Membranes," *J. Memb. Sci.*, **35**, 167 (1988).
Deen, W. M., "Hindered Transport of Large Molecules in Liquid-Filled Pores," *AIChE J.*, **33**, 1409 (1987).
Deiber, J. A., and W. R. Schowalter, "Modeling the Flow of Viscoelastic Fluids Through Porous Media," *AIChE J.*, **27**, 912 (1981).
Dutta, A., and R. A. Mashelkar, "Upper Bound on the Stress-Induced Migration Effect in Laminar Falling Film Flows of Dilute Polymer Solutions," *Chem. Eng. Commun.*, **39**, 277 (1985).
Gogarty, W. B., "Mobility Control with Polymer Solutions," *Soc. Pet. Eng. J.*, **7**, 161 (1967).
Goh, C. J., J. D. Atkinson, and N. Phan-Thien, "The Flow of Dilute Polymer Solution in a Narrow Channel. I. The Slip Effect in Simple Shear Flow," *J. Chem. Phys.*, **82**, 988 (1985a).
Goh, C. J., J. D. Atkinson, and N. Phan-Thien, "The Flow of Dilute Polymer Solution in a Narrow Channel. II. Plane Poiseuille Flow," *J. Chem. Phys.*, **82**, 3442 (1985b).
Goh, C. J., N. Phan-Thien, and J. D. Atkinson, "Bead-Spring Model for Adsorbed Polymer Chains in Shear Flow: Hydrodynamic Interaction," *J. Poly. Sci. Poly. Phys. Ed.*, **23**, 695 (1985c).
Grisafi, S., and P. O. Brunn, "Wall Effects in the Flow of a Dilute Polymer Solution: Numerical Results for Intermediate Channel Sizes," *J. Rheol.*, **33**, 47 (1989).

Guillot, G., L. Léger, and F. Rondelez, "Diffusion of Large Flexible Polymer Chains Through Model Porous Membranes," *Macromol.*, **18**, 2531 (1985).

Happel, J., and H. Brenner, *Low Reynolds Number Hydrodynamics*, Martinus Nijhoff, Boston (1983).

Jhon, M. S., and K. F. Freed, "Polymer Migration in Newtonian Fluids," *J. Poly. Sci. Poly. Phys. Ed.*, **23**, 955 (1985).

Jhon, M. S., G. Sekhon, and R. Armstrong, "The Response of Polymer Molecules in a Flow," *Adv. Chem. Phys.*, **66**, 153 (1987).

Kim, S., and S. J. Karrila, *Microhydrodynamics: Principles and Selected Applications*, Butterworth-Heinemann, Boston (1991).

Larson, R. G., "Flow-Induced Mixing, Demixing, and Phase Transitions in Polymeric Fluids," *Rheol. Acta*, **31**, 497 (1992).

Nitsche, L. C., "Fluctuation-Flipping Orbits of Freely-Draining Rigid Dumbbells in Converging-Diverging Pore Flows," *Chem. Eng. Commun.*, in press (1996).

Nitsche, L. C., and H. Brenner, "Hydrodynamics of Particulate Motion in Sinusoidal Pores Via a Singularity Method," *AIChE J.*, **36**, 1403 (1990).

Park, O. O., and G. G. Fuller, "Dynamics of Rigid and Flexible Polymer Chains in Confined Geometries: I. Steady Simple Shear Flow," *J. Non-Newtonian Fluid Mech.*, **15**, 309 (1984).

Phan-Thien, N., and M. M. K. Khan, "Flow of an Oldroyd-Type Fluid Through a Sinusoidally Corrugated Tube," *J. Non-Newtonian Fluid Mech.*, **24**, 203 (1987).

Rallison, J. M., and E. J. Hinch, "Do We Understand the Physics in the Constitutive Equation?," *J. Non-Newtonian Fluid Mech.*, **29**, 37 (1988).

Rey, A., J. J. Freire, and J. García de la Torre, "Brownian Dynamics of a Flexible Polymer. Internal Modes and Quasielastic Scattering Function," *J. Chem. Phys.*, **90**, 2035 (1989).

Rotne, J., and S. Prager, "Variational Treatment of Hydrodynamic Interaction in Polymers," *J. Chem. Phys.*, **50**, 4831 (1969).

Rudisill, J. W., and P. T. Cummings, "Brownian Dynamics Simulation of Model Polymer Fluids in Shear Flow. I. Dumbbell Models," *J. Non-Newtonian Fluid Mech.*, **41**, 275 (1992).

Sekhon, G., R. C. Armstrong, and M. S. Jhon, "The Origin of Polymer Migration in a Nonhomogeneous Flow Field," *J. Poly. Sci. Poly. Phys. Ed.*, **20**, 947 (1982).

Shafer, R. H., "Radial Migration of DNA Molecules in Cylindrical Flow. II. The Non-Draining Model and Possible Application to Fractionation," *Biophys. Chem.*, **2**, 185 (1974).

Shafer, R. H., N. Laiken, and B. H. Zimm, "Radial Migration of DNA Molecules in Cylindrical Flow. I. Theory of the Free-Draining Model," *Biophys. Chem.*, **2**, 180 (1974).

Shaqfeh, E. S. G., and D. L. Koch, "Polymer Stretch in Dilute Fixed Beds of Fibres or Spheres," *J. Fluid Mech.*, **244**, 17 (1992).

Stasiak, W., and C. Cohen, "Dilute Solutions of Macromolecules in a Rectilinear Poiseuille Flow," *J. Chem. Phys.*, **78**, 553 (1983).

Tirrell, M., and M. F. Malone, "Stress-Induced Diffusion of Macromolecules," *J. Poly. Sci., Poly. Phys. Ed.*, **15**, 1569 (1977).

Vorwerk, J., and P. O. Brunn, "Porous Medium Flow of the Fluid A1: Effects of Shear and Elongation," *J. Non-Newtonian Fluid Mech.*, **41**, 119 (1991).

Yamakawa, H., "Transport Properties of Polymer Chains in Dilute Solution: Hydrodynamic Interaction," *J. Chem. Phys.*, **53**, 436 (1970).

Manuscript received July 11, 1994, and revision received Apr. 19, 1995.